Prefrontal Regions Orchestrate Suppression of Emotional Memories via a Two-Phase Process

Prefrontal Regions Orchestrate Suppression of Emotional Memories via a Two-Phase Process

Brendan E. Depue,[1,2]* Tim Curran,[1,2,3] Marie T. Banich[1,2,3,4]

Whether memories can be suppressed has been a controversial issue in psychology and cognitive neuroscience for decades. We found evidence that emotional memories are suppressed via two time-differentiated neural mechanisms: (i) an initial suppression by the right inferior frontal gyrus over regions supporting sensory components of the memory representation (visual cortex, thalamus), followed by (ii) right medial frontal gyrus control over regions supporting multimodal and emotional components of the memory representation (hippocampus, amygdala), both of which are influenced by fronto-polar regions. These results indicate that memory suppression does occur and, at least in nonpsychiatric populations, is under the control of prefrontal regions.

One of the most controversial issues in psychology over the past 100 years is the degree to which memories can be manipulated, both whether they can be falsely created (1) and whether they can be suppressed. Although some researchers have provided initial evidence for memory suppression (2, 3), others claim that memory repression or suppression is a clinical myth in search of scientific support (4).

We hypothesized that evidence for memory suppression would be provided by activation below a fixation baseline in brain regions processing components of memory representation (5). We used the Think/No-Think paradigm (T/NT) of Anderson and colleagues, in which individuals attempt to elaborate a memory by repetitively thinking of it (T condition) or to suppress a memory by repetitively not letting it enter consciousness (NT condition) (2, 3). Our recent T/NT work,

using faces as cues and pictures as targets, suggests that the impact of exerting control is larger for emotional than for nonemotional information (6). Because of these findings, as well as the clinical relevance of intrusive negative images in posttraumatic stress disorder (PTSD) and obsessive-compulsive disorder (OCD) (7–9), we used negative pictures known to activate the visual cortex as memory targets (10). In both monkeys (11) and humans (10), retrieval of memories involves the same regions of the brain that are involved in encoding a memory (12, 13). Thus, we used the degree of activation in the hippocampus, amygdala, and visual processing areas that are known to be involved in the creation and retrieval of emotional memories (14, 15)—to determine whether memory suppression involves inhibition of the neural machinery underlying memory processing.

Two aspects of our version of the T/NT paradigm were important (Fig. 1A). First, the experimental phase included fixation items that acted as a low-level baseline of brain activity to

[1]Department of Psychology, University of Colorado, Boulder, CO 80309, USA. [2]Center for Neuroscience, University of Colorado, Boulder, CO 80309, USA. [3]Institute of Cognitive Science, University of Colorado, Boulder, CO 80309, USA. [4]Department of Psychiatry, University of Denver Health Sciences, Denver, CO 80208, USA.

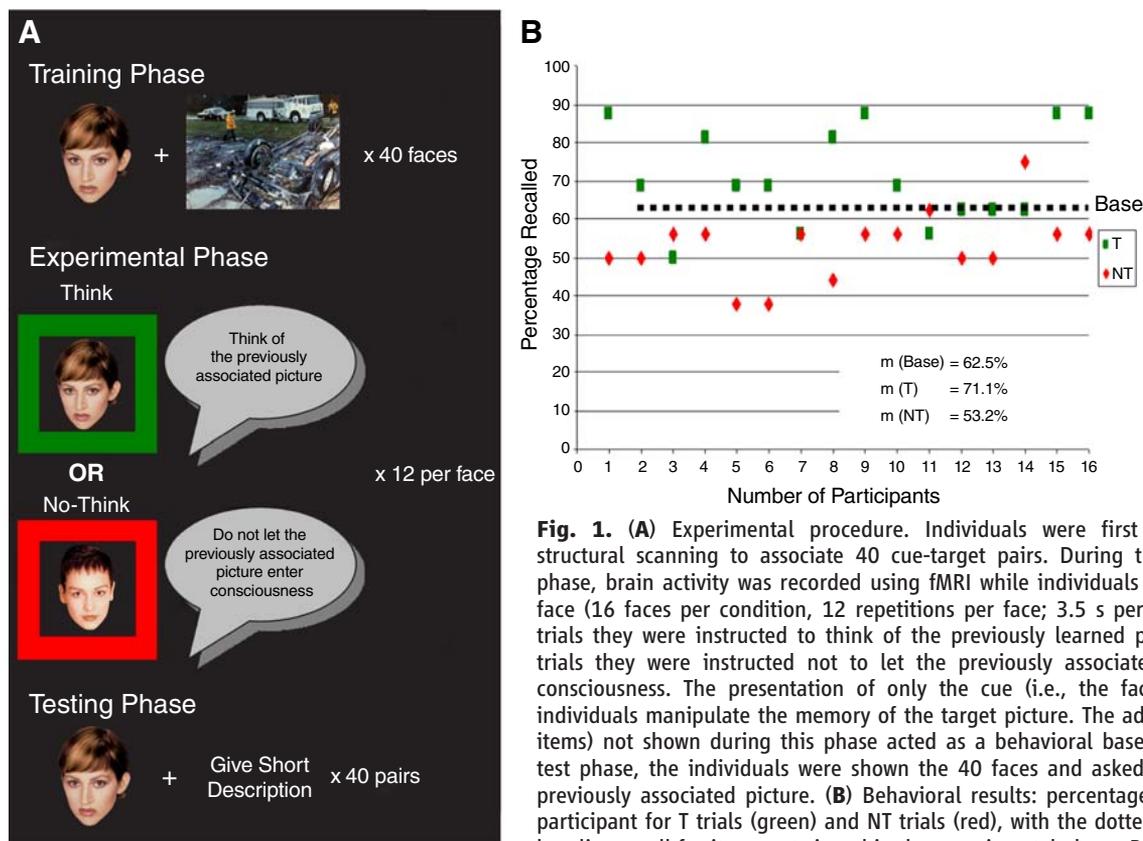*To whom correspondence should be addressed. E-mail: depue@colorado.edu

Fig. 1. (**A**) Experimental procedure. Individuals were first trained during structural scanning to associate 40 cue-target pairs. During the experimental phase, brain activity was recorded using fMRI while individuals viewed only the face (16 faces per condition, 12 repetitions per face; 3.5 s per face). On some trials they were instructed to think of the previously learned picture; on other trials they were instructed not to let the previously associated picture enter consciousness. The presentation of only the cue (i.e., the face) ensures that individuals manipulate the memory of the target picture. The additional faces (8 items) not shown during this phase acted as a behavioral baseline. During the test phase, the individuals were shown the 40 faces and asked to describe the previously associated picture. (**B**) Behavioral results: percentage recall for each participant for T trials (green) and NT trials (red), with the dotted line indicating baseline recall for items not viewed in the experimental phase. Recall differed for T and NT items [$t(15) = -4.29$, $P = 0.0006$] because of a trend for greater recall in the T condition [$t(15) = 1.49$, $P = 0.07$] and a significant reduction in recall in the NT condition [$t(15) = -2.28$, $P = 0.02$], calculated relative to baseline.

determine whether activity in the regions of interest (ROIs) actually decreased (5). Although Anderson and colleagues (2) demonstrated the involvement of prefrontal regions in cognitive control over memory, they examined the contrast between activation on NT and T trials without reporting fixation baseline contrasts, making it difficult to associate activity with a specific condition (e.g., T or NT).

Second, in the experimental phase, each face was shown 12 times with the presentation of the faces pseudo-randomly intermixed. Although in our previous study (6) memory increased linearly with the number of times cognitive control was exerted for T trials, this was not the case for NT trials. Hence, we divided our data into quartiles (three repetitions per cue during each quartile) to determine whether the neural mechanisms involved in memory suppression change with repeated attempts.

The behavioral results shown in Fig. 1B indicated that individuals effectively suppressed memory. To investigate the neural basis of this effect, we first analyzed the functional magnetic resonance imaging (fMRI) data for instances of NT > T—that is, significantly greater activity for NT trials than for T trials—irrespective of recall accuracy (5). Additionally, because we were specifically interested in effective control over memory, we examined this same contrast only for NT trials in which the picture was forgotten (NTf) and on T trials in which it was remembered (Tr). Brain areas are discussed according to their putative functional roles: (i) cognitive control, (ii) sensory representation of memory, and (iii) memory processes and emotional components of memory.

Sources and sites of cognitive control. Prefrontal regions, right-sided and spanning BA 8, 9/46, 47, and BA 10, exhibited NT > T contrast. A conjunction analysis indicated that these differences resulted from an increase in activity for NT trials rather than a decrease in activation for T trials relative to baseline (Fig. 2A), which suggests that these regions are specifically involved in controlling the suppression of emotional memories.

Next, we sought to determine which regions support components of the memory representation. These regions showed condition-specific changes, which we defined as yielding not only a significant difference for the NT > T contrast but also a negative signal change for NT trials and, conversely, a positive signal change for T trials, relative to baseline. Brain areas underlying the sensory representation of memory that showed such an effect were the visual cortex, including bilateral BA17, BA18, and BA37 [fusiform gyrus (FG); Fig. 2B], and the pulvinar nucleus of the thalamus (Pul; Fig. 2B). Suppression of emotional memories thus involved decreased activity in sensory cortices that are normally active when memories are being retrieved, as well as in regions (i.e., Pul) that play a role in gating and modulating attention toward or away from visual stimuli (16, 17).

Brain areas involved in memory processes and emotional components of memory representation that exhibited significant condition-specific activity were the hippocampal complex (Hip) and the amygdala (Amy; Fig. 2C), which are strongly involved in emotional learning and memory (18, 19), as would be required by the face-picture association in our paradigm. Hence, the suppression of emotional memory also involved suppression of memory processes and emotional aspects of the memory representation.

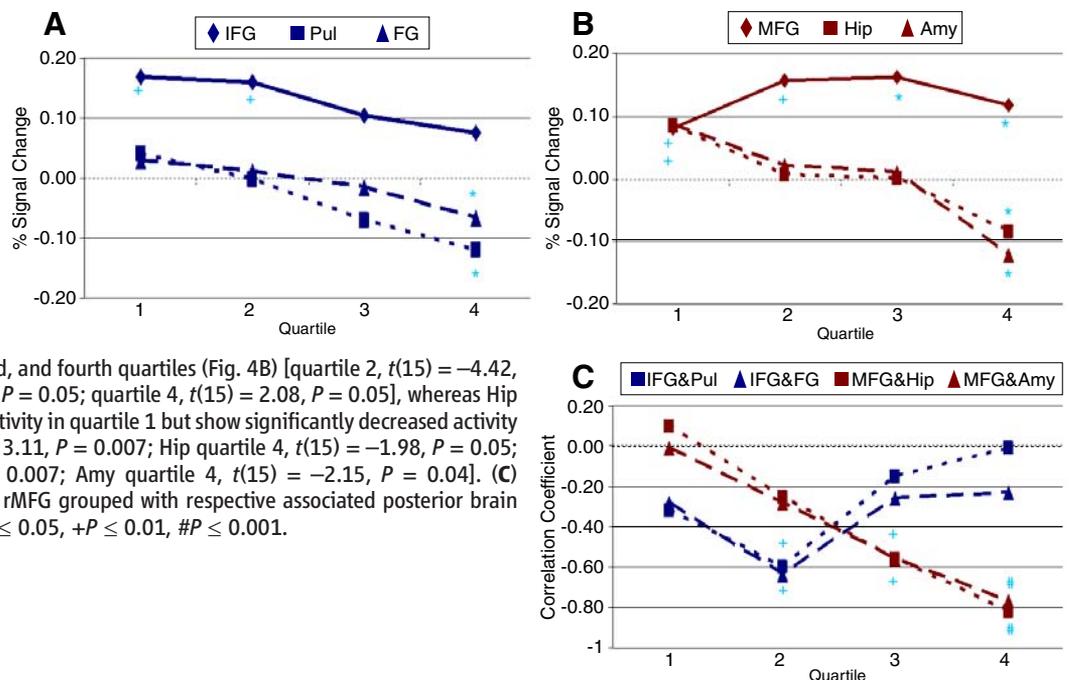**Two phases of memory suppression.** We next examined how brain activity changed with

Fig. 2. Functional activation of brain areas involved in (**A**) cognitive control, (**B**) sensory representations of memory, and (**C**) memory processes and emotional components of memory (rSFG, right superior frontal gyrus; rMFG, right middle frontal gyrus; rIFG, right inferior frontal gyrus; Pul, pulvinar; FG, fusiform gyrus; Hip, hippocampus; Amy, amygdala). fMRI data were analyzed using a hemodynamic response function–convolved epoch; statistical parameter maps (SPMs) were thresholded on a voxelwise basis at $Z = 2.81$, $P = 0.005$. To adjust for false positive errors on an area-of-activation basis, we set a clusterwise threshold at $P = 0.05$ (cluster size of 120) as determined by the Analysis of Functional NeuroImages program AlphaSim. Red indicates greater activity for NT trials than for T trials; blue indicates the reverse. Conjunction analyses revealed that areas seen in blue are the culmination of increased activity for T trials above baseline as well as decreased activity of NT trials below baseline.
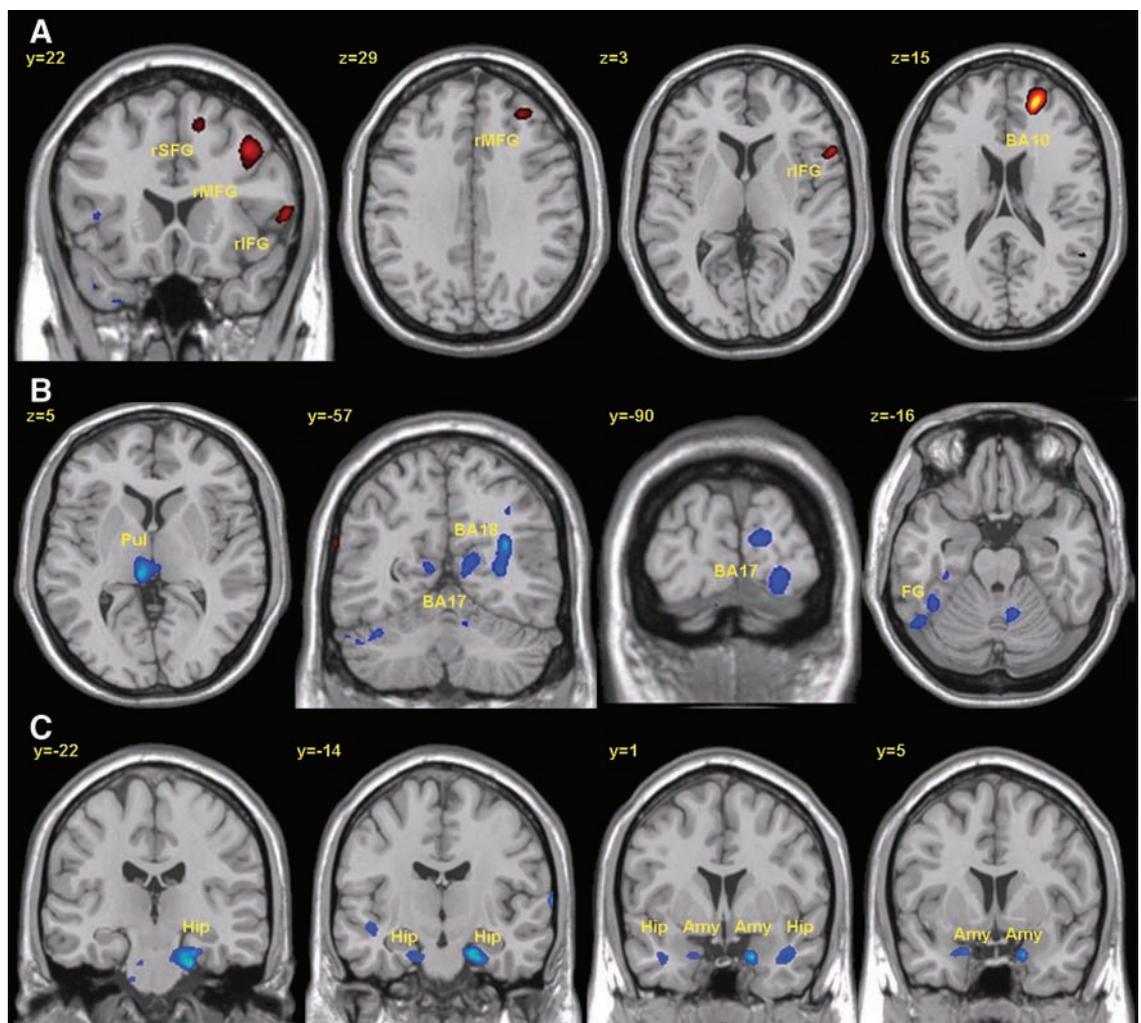
increased attempts at cognitive control, over trials, as well as covariation of prefrontal activation and the two putative sets of posterior cortex (sensory areas, Amy-Hip complex). This was accomplished by dividing the 12 attempts at cognitive control into quartiles (three repetitions per quartile). We then plotted percent signal change (ΔS) across the quartiles of each brain area that showed differential activation for NT trials relative to T trials (5).

Two patterns of temporal change in activation were observed, each associated with different groupings of prefrontal and posterior brain areas. The two groupings were composed of (i) right inferior frontal gyrus (rIFG), Pul, and FG, and (ii) right middle frontal gyrus (rMFG), Hip, and Amy. Unique temporal patterns of prefrontal cortex (PFC) influence on posterior brain regions were observed for each group. rIFG showed early activation in the time course of suppression, which lasted through the second quartile of repetitions, and then a decreased level of activation during the last two quartiles (Fig. 3A). Activity of Pul and FG followed a similar time course of ΔS, which lagged behind that for rIFG. To express quantitatively the relationship in activation between these brain areas as a function of time, we plotted the correlations of activation of rIFG with Pul and FG, respectively, as a function of quartile (Fig. 3C). Greater activity in rIFG in the second quartile was significantly associated with decreased activity in Pul and FG during the second quartile, but showed no significant relation for later quartiles (20). This correlation pattern is consistent with the temporal pattern of ΔS: The apparent rIFG inhibition of its associated brain regions begins early, in the first quartile, reaches maximum in the second quartile, and is greatly reduced thereafter.

In contrast to rIFG, rMFG activation increased later and remained active. Activity in Hip and Amy appeared to follow that of rMFG in reverse: In the first quartile, activity was significantly above baseline, but it decreased steadily to reach significance below baseline by the fourth quartile (Fig. 3B). Increased activity in rMFG did not predict activity in Hip and Amy in the first or second quartiles, but did so significantly in the third and fourth quartiles (Fig. 3C). This covariation pattern suggests that rIFG and rMFG suppress different aspects of memory processing during different temporal phases.

To assess the linkage between Hip activation and memory, we performed a subsequent memory analysis (remembered versus forgotten) on Hip activation during the fourth quartile, when the effects of cognitive control were largest. We found a linear decrease of activity in Hip: Tr > Tf > baseline > NTr > NTf (5), with only that of NT trials below baseline. Further analyses showed that activity of rMFG and Hip correlated with behavioral success at suppression (5). Taken together with the previous data, these findings suggest that rMFG modulates activity in Hip, which is directly related to behavioral success. These data replicated the finding of Anderson and colleagues, so the relationship between prefrontal and hippocampal regions may well be involved in suppressing memory recall.

Higher-order orchestration of memory suppression. Only one prefrontal region, BA 10, exhibited activity across the entire experimental phase (Fig. 4A). Because this region receives minimal sensory input and is predominantly connected with other prefrontal areas, we inspected its relationship with rIFG and rMFG for each quartile. The maximal correlation between

BA10 and each of the prefrontal regions was observed in the quartile preceding the maximal correlation between rIFG and rMFG and their respectively associated brain regions (Fig. 4, B to D). This pattern suggests that activity in BA10 modulates activity in rIFG and rMFG, which in turn modulates activity in posterior regions. This result is consistent with recent research suggesting that activity in BA10 increases with task complexity and is involved in other aspects of higher-order cognition, such as monitoring of internal states, memory retrieval, emotional processes, coordination of higher-level goals, and modulating other areas of PFC to attain these goals (21, 22).

Conclusion. Our finding of below-baseline activation in brain areas related to sensory representation (Pul, FG) and memory (Hip, Amy) for emotional stimuli during NT trials is consistent with the operation of an active process of suppression. Furthermore, our findings are less consistent with two sets of alternative interpretations of responses in behavior and brain activation that we observe on NT trials. One alternative explanation is replacement, in which participants think of a new cue-target association or substitute an alternate memory to create distraction from the target memory (23). However, the generation of a new associate would be associated with activation, not deactivation below baseline of sensory and memory representations to represent and encode the new association. In essence, replacement would manifest functionally in brain activations as in T trials.

A second alternative suggests that reduced recall on NT trials involves disengagement with the stimuli (e.g., momentary mind-wandering or introspection), because in some studies BA10 activation has been correlated with internally fo-

---

Fig. 3. Time course of percentage signal change (ΔS) relative to baseline for the two regional groupings. (**A**) rIFG shows significantly increased activity only for the first and second quartiles [quartile 1, $t(15) = 3.65$, $P = 0.001$; quartile 2, $t(15) = 2.66$, $P = 0.01$], whereas the activities of Pul and FG decrease to significantly below baseline during quartile 4 [Pul, $t(15) = -2.11$, $P = 0.05$; FG, $t(15) = -1.96$, $P = 0.05$]. (**B**) rMFG displays significantly elevated activity during the second, third, and fourth quartiles (Fig. 4B) [quartile 2, $t(15) = -4.42$, $P = 0.0005$; quartile 3, $t(15) = 2.10$, $P = 0.05$; quartile 4, $t(15) = 2.08$, $P = 0.05$], whereas Hip and Amy initially exhibit increased activity in quartile 1 but show significantly decreased activity by quartile 4 [Hip quartile 1, $t(15) = 3.11$, $P = 0.007$; Hip quartile 4, $t(15) = -1.98$, $P = 0.05$; Amy quartile 1, $t(15) = 3.11$, $P = 0.007$; Amy quartile 4, $t(15) = -2.15$, $P = 0.04$]. (**C**) Correlation coefficients for rIFG and rMFG grouped with respective associated posterior brain regions as a function of quartile. *$P \leq 0.05$, +$P \leq 0.01$, #$P \leq 0.001$.

cused attention. However, we found that BA10 activity precedes and covaries with the activity of two separate prefrontal areas that are initiated at different temporal points in the process of suppressing activation in two different sets of posterior brain regions. This time-phased, region-specific activity pattern of BA10 is more complex than that expected for simple mind-wandering during NT trials, and is more consistent with BA10's proposed role of orchestration of multiple prefrontal processes involved in guiding complex tasks (21, 22).

Our findings suggest that the suppression of emotional memory involves at least two pathways with staggered phases of their modulatory influence. The first pathway involves cognitive control by rIFG over sensory components of memory representation, as evidenced by reduced activity in FG and Pul. This finding is consistent with computational models that posit that activation and inhibition of the thalamus is a critical means of gating working memory information (24). A second pathway involves cognitive control by rMFG over memory processes and emotional components of memory representation via modulation of Hip and Amy (2, 25). The overall timing of these suppression effects appears to be orchestrated by a modulatory influence of BA10, first over rIFG, then over rMFG. Further research is needed to determine the extent to which the two pathways act independently or interactively.

Our findings also provide insight into the potential neurocognitive mechanisms by which emotional memories are suppressed. Our data are consistent with the idea that initial memory

suppression is most readily accomplished by prefrontal modulation of activity in sensory cortices that is likely to recreate the sensory percept. This process, however, does not predict subsequent behavioral recall and may be a "late-correction" mechanism (26) to suppress prepotent activity in sensory cortices generated as a result of viewing the cue. In contrast, activity of rMFG (over all quartiles) and Hip (during the last quartile) predicts behavioral suppression (5). This suppression process may reduce access to the memory itself, by blocking Hip and Amy activity needed for retrieval of the emotional memory. However, this mechanism becomes effective only after repeated attempts at control, as shown by the increased correlation in activity between rMFG-Hip and rMFG-Amy over quartiles (Fig. 3C). Once successful suppression of hippocampal activity is achieved, the need to invoke the "late-correction" process apparently decreases, as reflected in the decreased rIFG-Pul and rIFG-FG correlations.

Our data also provide an intriguing hint that, as suggested in clinical practice, it is necessary to "revisit" an emotionally distressing memory before it can be controlled. We found that early in the course of suppression (during quartiles 1 and 2), greater Hip activity was observed for NTf trials than NTr trials, as was also found by Anderson *et al.* in nontemporal analyses (2, 5). We speculate that memories that activate Hip to a greater degree are more amenable to cognitive control because they are more elaborated and may provide increased access. By the fourth quartile, activation in Hip for NTf trials (but not NTr trials) is significantly below baseline, indi-

cating that Hip activity has been effectively suppressed.

At a broader level, our findings extend research suggesting that prefrontal brain areas associated with inhibitory mechanisms (BA 10 and superior, inferior, and middle FG) are lateralized predominantly to the right hemisphere (27, 28). We have shown the involvement of these areas in the suppression of emotional memories, which replicates current literature suggesting that these areas are active in the suppression of emotional reactivity (29, 30). Activity in these brain areas, along with inhibition over Hip and Amy, suggests that suppression of emotional memories may use mechanisms similar to those used in emotion regulation. Thus, various right-lateralized PFC areas may be involved in coordinating suppression processes across many behavioral domains, including memory retrieval, motor processes, feelings of social rejection, self motives, and state emotional reactivity (27–32).

Our findings may have implications for therapeutic approaches to disorders involving the inability to suppress emotionally distressing memories and thoughts, including PTSD, phobias, ruminative depression/anxiety, and OCD. They provide the possibility for approaches to controlling memories by suppressing sensory aspects of memory and/or by strengthening cognitive control over memory and emotional processes through repeated practice. Refinement of therapeutic procedures based on these distinct means of manipulating emotional memory might be an exciting and fruitful development in future clinical research.

Fig. 4. (**A**) Time course of percent signal change for BA10, rIFG, and rMFG. (**B**) Correlations of rBA10 with rIFG and rMFG as a function of quartiles of suppression repetitions. (**C**) Correlations of BA10 with rIFG, rIFG with Pul, and rIFG with FG as a function of quartiles of suppression repetitions. (**D**) Correlations of BA10 with rMFG, rMFG with Hip, and rMFG with Amy as a function of suppression repetitions. Arrows in (C) and (D) indicate a preceding orchestration of control. For the quartile in which the correlation was maximal, greater activity in BA10 was associated with significantly increased activity in rIFG ($r = 0.56$, $P = 0.03$) and rMFG ($r = 0.77$, $P = 0.001$), but not with other brain areas [Pul, $r = -0.16$; FG, $r = -0.16$; Hip, $r = -0.22$; Amy, $r = -0.09$; $Ps > 0.40$ (5)]. *$P \leq 0.05$, +$P \leq 0.01$, #$P \leq 0.001$.
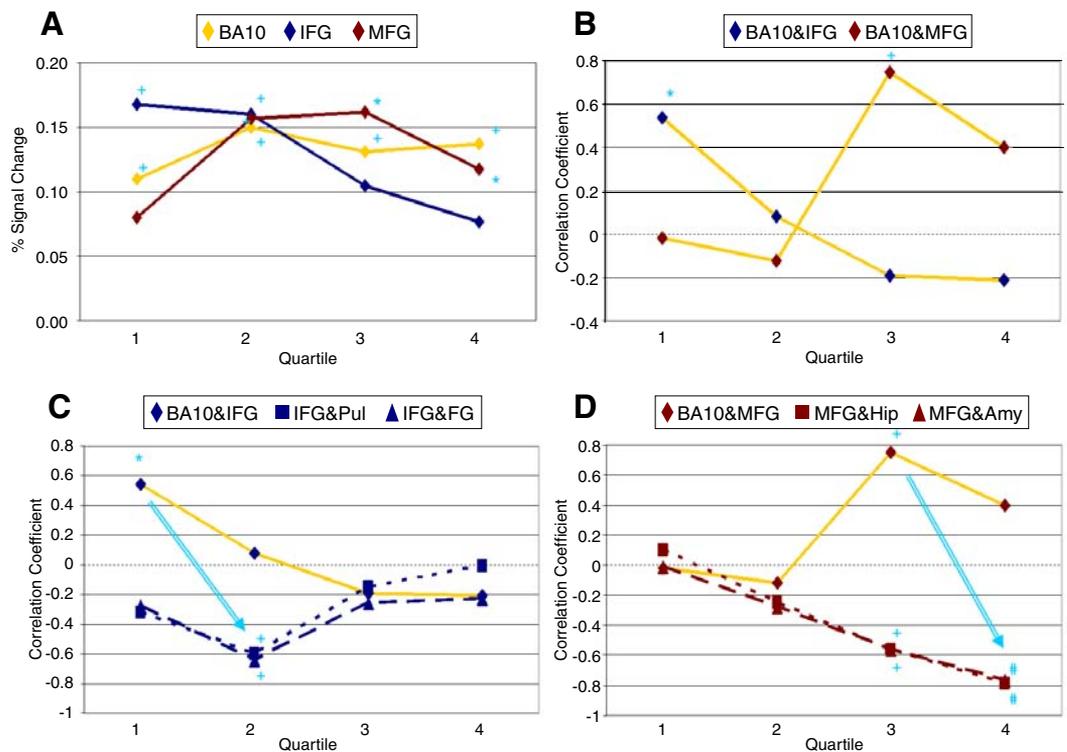
Our results suggest that effective voluntary suppression of emotional memory only develops with repeated attempts to cognitively control posterior brain areas underlying instantiated memories. In this sense, memory suppression may best be conceived as a dynamic process in which the brain acquires multiple modulatory influences to reduce the likelihood of retrieving unwanted memories.

References and Notes

1. E. Loftus, *Neuroscience* **4**, 231 (2003).
2. M. C. Anderson *et al.*, *Science* **303**, 232 (2004).
3. M. C. Anderson, C. Green, *Nature* **410**, 366 (2001).
4. J. F. Kihlstrom, *Trends Cognit. Sci.* **6**, 502 (2002).
5. See supporting data on *Science* Online.
6. B. E. Depue, M. T. Banich, T. Curran, *Psychol. Sci.* **17**, 441 (2006).
7. B. A. van der Kolk, J. A. Burbridge, J. Suzuki, *Ann. N.Y. Acad. Sci.* **821**, 99 (1997).
8. B. A. van der Kolk *et al.*, *Am. J. Psychiatry* **153**, 83 (1996).
9. C. Purdon, *Behav. Res. Ther.* **37**, 1029 (1999).
10. P. J. Lang *et al.*, *Psychophysiology* **35**, 199 (1998).
11. E. T. Rolls, *Hum. Neurobiol.* **3**, 209 (1984).
12. S. M. Kosslyn, W. L. Thompson, in *The New Cognitive Neurosciences*, M. S. Gazzaniga, Ed. (MIT Press, Cambridge, MA, ed. 2, 2000), pp. 975–985.
13. C. L. Raye *et al.*, *Cortex* **43**, 135 (2007).
14. A. D. Wagner *et al.*, *Neuroimage* **14**, 1337 (2001).
15. J. L. McGaugh, *Science* **287**, 248 (2000).
16. S. Kastner *et al.*, *J. Neurophysiol.* **91**, 438 (2004).
17. S. Kastner *et al.*, *Science* **282**, 108 (1998).
18. S. Hamann, *Trends Cognit. Sci.* **5**, 394 (2001).
19. E. A. Phelps, *Curr. Opin. Neurobiol.* **14**, 198 (2004).
20. Our activation of FG has been established to be different (more posterior/medial) from the activation of the fusiform face area (FFA) commonly observed in face perception studies (*33*).
21. K. Sakai, R. E. Passingham, *J. Neurosci.* **26**, 1211 (2006).
22. N. Ramnani, A. M. Owen, *Nat. Rev. Neurosci.* **5**, 184 (2004).
23. P. T. Hertel, G. Calcaterra, *Psychonom. Bull. Rev.* **12**, 484 (2005).
24. R. C. O'Reilly, *Science* **314**, 91 (2006).
25. M. Beauregard, J. Lévesque, P. Bourgouin, *J. Neurosci.* **21**, RC165 (2001).
26. L. L. Jacoby, C. M. Kelley, B. D. McElree, in *Dual-Process Theories in Social Psychology*, S. Chaiken, Y. Trope, Eds. (Guilford, New York, 1999), pp. 383–400.
27. H. Garavan, T. J. Ross, E. A. Stein, *Proc. Natl. Acad. Sci. U.S.A.* **96**, 8301 (1999).
28. A. R. Aron, T. W. Robbins, R. A. Poldrack, *Trends Cognit. Sci.* **8**, 170 (2004).
29. K. N. Ochsner *et al.*, *J. Cognit. Neurosci.* **14**, 1215 (2002).
30. N. I. Eisenberger, M. D. Lieberman, K. D. Williams, *Science* **302**, 290 (2003).
31. H. L. Urry *et al.*, *J. Neurosci.* **26**, 4415 (2006).
32. D. Knoch, A. Pascual-Leone, K. Meyer, V. Treyer, E. Fehr, *Science* **314**, 829 (2006); published online 4 October 2006 (10.1126/science.1129156).
33. I. Gautier *et al.*, *Nat. Neurosci.* **3**, 191 (2000).
34. We thank Y. Du, D. Singel, and R. Freedman for assistance in functional imaging, and three anonymous reviewers for their critical insights. Supported by the Graduate School, the Vice-Chancellor for Research, and the Institute of Cognitive Science at the University of Colorado at Boulder (M.T.B.).

Scattering and Interference in Epitaxial Graphene

G. M. Rutter,[1] J. N. Crain,[2] N. P. Guisinger,[2] T. Li,[1] P. N. First,[1]* J. A. Stroscio[2]*

A single sheet of carbon, graphene, exhibits unexpected electronic properties that arise from quantum state symmetries, which restrict the scattering of its charge carriers. Understanding the role of defects in the transport properties of graphene is central to realizing future electronics based on carbon. Scanning tunneling spectroscopy was used to measure quasiparticle interference patterns in epitaxial graphene grown on SiC(0001). Energy-resolved maps of the local density of states reveal modulations on two different length scales, reflecting both intravalley and intervalley scattering. Although such scattering in graphene can be suppressed because of the symmetries of the Dirac quasiparticles, we show that, when its source is atomic-scale lattice defects, wave functions of different symmetries can mix.

Built of a honeycomb of sp^2-bonded carbon atoms, graphene has a linear, neutrino-like energy spectrum near the Fermi energy, E_F. This results from the intersection of electron and hole cones in the graphene band structure at the Dirac energy, E_D. The linear energy dispersion and concomitant topological constraints give rise to massless Dirac quasiparticles in graphene, with energy-independent propagation speed $v_F \approx 10^6$ m/s (where v_F is the Fermi velocity). Distinctive symmetries of the graphene wave functions lead to unusual quantum properties, such as an anomalous integer quantum Hall effect (*1*, *2*) and weak antilocalization (*3*, *4*), that have spurred an intense scientific interest in graphene (*5*). Bilayer graphene (*5*–*7*) is equally distinctive: Quasiparticle states are chiral (*6*) with Berry's phase 2π for the bilayer versus π for the monolayer (*6*). High carrier mobilities, chemical inertness, and the two-dimensional (2D) nature of graphene make it a promising candidate for future electronic-device applications (*1*, *2*, *5*, *8*, *9*). In particular, graphene grown epitaxially on SiC substrates and patterned via standard lithographic procedures has been proposed as a platform for carbon-based nanoelectronics and molecular electronics (*8*, *9*).

Epitaxial graphene was grown on the silicon-terminated (0001) face of high-purity semi-insulating 4H-SiC by thermal desorption of silicon at high temperatures (*8*, *10*). This method produces an electron-doped graphene system, with the Fermi level 200 to 400 meV above E_D.

The data that we present were obtained from a region identified as bilayer graphene (*11*). Scanning tunneling microscopy (STM) measurements were performed in a custom-built ultrahigh-vacuum, low-temperature instrument. We measured the scanning tunneling spectroscopy (STS) differential conductance dI/dV (where I is current and V is voltage) with lock-in detection by applying a small modulation to the tunnel voltage at ≈ 500 Hz. Differential conductance maps were obtained by recording an STS spectrum at each spatial pixel in the topographic measurement. All measurements reported here were taken at 4.3 K.

STM topographic images (Fig. 1) show the atomic structure and different types of disorder for epitaxial graphene on SiC(0001). At the atomic scale, the graphene is imaged as a triangular lattice (Fig. 1B), characteristic of imaging only one of the two graphene sublattices. Superimposed on this atomic structure is a modulation period of ≈ 2 nm caused by a reconstruction of the SiC interface beneath the graphene: a SiC "6 × 6" superstructure (*12*). Survey images reveal two categories of defects. Type A defects, such as mounds (red arrow in Fig. 1A), have an unperturbed graphene structure that is continuous, akin to a blanket. These defects are due to irregularities in the interface layer between graphene and the SiC bulk. In contrast, type B defects are atomic defects within the graphene lattice itself (Fig. 1, A, C, and D) and are accompanied by strong distortions in the local lattice images. These distortions are of electronic origin and are accompanied by large increases in the local density of states (LDOS) at the defect site (*13*, *14*). Quasiparticle scattering from type B defects gives rise to spectacular patterns in the topographic images (Fig. 1, C and D) resulting

[1]School of Physics, Georgia Institute of Technology, Atlanta, GA 30332, USA. [2]Center for Nanoscale Science and Technology, National Institute of Standards and Technology, Gaithersburg, MD 20899, USA.

*To whom correspondence should be addressed. E-mail: joseph.stroscio@nist.gov (J.A.S.); first@physics.gatech.edu (P.N.F.)